AIAA AVIATION Forum
17-21 June 2019, Dallas, Texas
AIAA Aviation 2019 Forum

10.2514/6.2019-3194

Altitude-Controlled Light Gas Balloons for Venus and Titan Exploration

Jeffery L. Hall,[1] Jonathan M. Cameron,[2] Michael T. Pauken,[3] Jacob S. Izraelevitz[4], Mitchell W. Dominguez,[5] Kristopher T. Wehage[6]
Jet Propulsion Laboratory, California Institute of Technology, Pasadena, CA., 91109, USA.

Abstract

This paper assesses the use of variable altitude light gas balloons for the robotic exploration of Venus and Titan. Helium is the buoyancy gas chosen for this study. Inspired by recent terrestrial examples, we consider three different types of helium-filled balloons that control their altitude over a specified range, each with a different modulation technique. These techniques are: pumping helium between a non-pressurized "zero-pressure" balloon and a pressurized reservoir to adjust buoyancy; pumping air into a pressurized reservoir to adjust weight; and changing the volume of the helium balloon through direct mechanical compression to adjust buoyancy. Theoretical derivations are presented for the limiting case of equal balloon and atmospheric gas temperatures that show two linear scaling relationships depending on the balloon option. The reservoir pressure linearly scales with atmospheric temperature for the pumped helium and pumped air options, but scales linearly with atmospheric pressure for the mechanical compression option. Simplified point designs are presented for Venus and Titan mission scenarios that quantify differences between the aerobot options based on vehicle mass, altitude stability, altitude range, and the energy required to change altitude. The data show that the pumped helium balloon option has the least vehicle mass and lowest energy consumption to change altitude for the Venus mission scenario, but it also has the highest amount of helium pressurization. The pumped helium balloon option also has the least vehicle mass and lowest energy consumption to change altitude for the Titan mission scenario; however, all Titan options require an order of magnitude less balloon mass and energy to change altitude compared to the Venus mission scenario, indicating that the mass and energy differences are not a significant discriminator for Titan. Preliminary results are presented for a dynamics-based simulation model for a Venus pumped helium balloon using the Dynamics Simulator for Entry, Descent and Surface Landing (DSENDS) tool. These results show good agreement with the simplified neutral buoyancy calculations.

Introduction

A recent NASA-sponsored study on Venus Aerial platforms[1] assessed a wide assortment of aerial vehicle types for the future exploration of Venus. The study concluded that long-duration

[1] Assistant Section Manager, Mobility and Robotic Systems Section, AIAA Associate Fellow.
[2] Senior Engineer, Mobility and Robotic Systems Section
[3] Senior Research Technologist, Thermal and Materials Engineering Section
[4] Robotics Technologist, Mobility and Robotic Systems Section
[5] Engineering student intern, Mobility and Robotic Systems Section
[6] Robotics Technologist, Mobility and Robotic Systems Section

variable altitude balloons based on lighter-than-air vehicle technology could provide a significant science return for modest investments in technology development. This conclusion rested in part on the successful development and flight-testing in recent years of terrestrial balloons that utilize altitude-control functionality to effect trajectory control by riding winds with different directions at different altitudes. This includes the Google Loon balloons[2], The World View Stratolite balloons[3], and the Voss Controlled Meteorological (CMET) balloons.[4] These vehicles consume electrical power to change altitude via gas pumping instead of traditional balloon techniques of ballast drops and buoyancy gas venting that permit flights of only limited duration before exhausting the consumables. Adaptation of this terrestrial technology for use at Venus requires a vehicle design that accommodates the different flight environment at Venus, notably the sulfuric acid clouds and the high atmospheric temperatures and pressures found below the clouds. The extent of technology investment is similar for adapting variable altitude balloon technology for Saturn's moon Titan, where the environment features cryogenically cold atmospheric temperature and hydrocarbon aerosols.

Venus and Titan applications tend to be more interested in the ability of these balloons to scientifically explore different altitudes as compared to current terrestrial balloons that use altitude control mostly as a means to effect trajectory control. This is particularly true for the Venus upper atmosphere where there is a very high wind speed of 70+ m/s in the equatorial direction that carries the vehicle around the planet in approximately 5 to 6 Earth-days. No winds of the opposite direction exist to balance this and enable the kind of station keeping typically desired for Earth applications. However, there is uncertainty in the magnitude, direction and variability of the meridional (poleward) wind component at Venus, and it may be that some latitude control can be exercised by variable altitude balloons depending on the nature of those winds as predicted and/or discovered in real time. The opportunities for trajectory control at Titan are much more promising given the complex multi-directional nature of winds as predicted from global circulation models. Prior work has in fact quantified the ability of non-propelled variable altitude balloons to target overflights of locations at a global scale on Titan.[5]

The term "aerobot" (AERObotical roBOT) has been used for a robotic balloon vehicle that autonomously exercises trajectory and/or altitude control.[6] We will use that term in this paper to refer to the complete robotic vehicle comprising the balloon, payload and software required to operate in a highly autonomous fashion at Venus and Titan.

This paper discusses the different types of light gas variable altitude aerobots and presents some underlying theory governing the design of such vehicles. Point designs based on helium buoyancy gas are presented for both Venus and Titan missions, both to fix ideas and to enable comparisons between the different aerobot types on the basis of vehicle mass and energy consumption to effect a given altitude change. These point designs are based on equilibrium altitude calculations with simplifying assumptions. At the end of the paper we also present some preliminary results of more detailed dynamics simulations of a Venus aerobot point design that corroborates some results from the simplified equilibrium analysis.

Light Gas Variable Altitude Aerobot Options

We consider three main types of helium aerobots for Venus and Titan:

1. Pumped Helium (PH), which modulates buoyancy in a tandem balloon vehicle by pumping helium from an unpressurized balloon into a separate pressurized balloon.
2. Throughout this paper we use the term "zero pressure" to refer to a nominally unpressurized balloon, and the term "superpressure" to refer to a pressurized balloon. In the case of this PH aerobot, the superpressure balloon acts as a constant volume reservoir.
3. Air Ballast (AB), which modulates the weight of the vehicle by pumping atmospheric gas (air) into and out of a pressurized container. This container is typically a superpressure balloon rather than an actual rigid tank structure.
4. Mechanical Compression (MC), which mechanically changes the volume of a balloon thereby directly changing the buoyancy provided by a fixed mass of helium gas.

These types of aerobots are illustrated in Fig. 1. There are sub-types for the PH and AB options that differentiate between two separate balloons or one balloon with an internal chamber or dividing bladder. Note that the PH type of balloon is called a "differential expansion balloon" in the Voss *et al*. paper.[4] The Google Loon balloon[2] is an Air Ballast balloon of sub-type 2, the

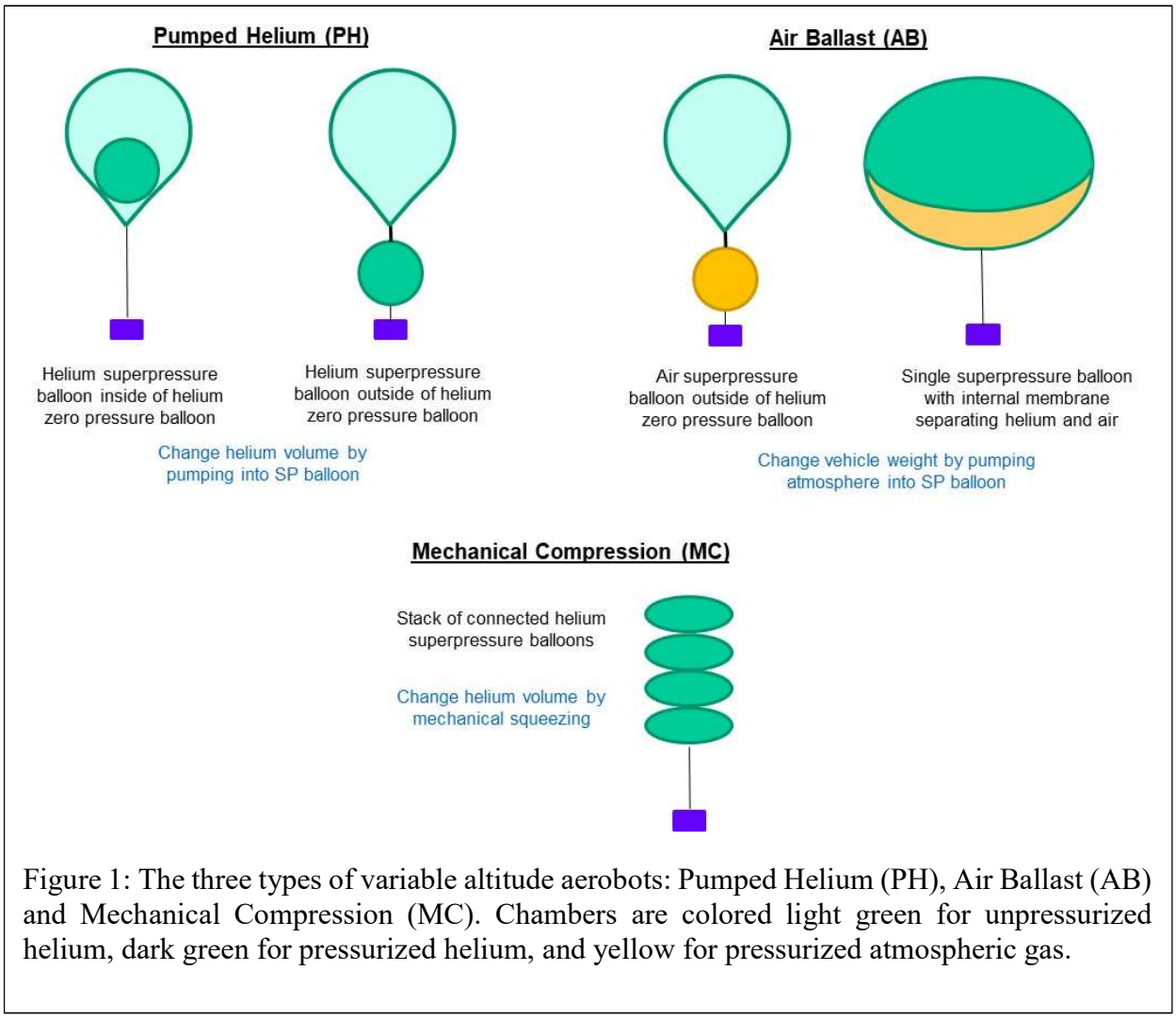

Figure 1: The three types of variable altitude aerobots: Pumped Helium (PH), Air Ballast (AB) and Mechanical Compression (MC). Chambers are colored light green for unpressurized helium, dark green for pressurized helium, and yellow for pressurized atmospheric gas.

WorldView Stratolite balloon[3] is an Air Ballast balloon of sub-type 2, and the CMET balloon[4] is a pumped helium balloon of sub-type 1. An example Mechanical Compression balloon is described in a patent application by Thin Red Line Aerospace.[7] Although helium is specified in this taxonomy, it is certainly possible to substitute hydrogen or another buoyancy gas.

The Key Role of Superpressure in Aerobot Design

The PH and AB balloons require a pump to move gas (helium or air) into the pressurized reservoir in order to achieve a lower equilibrium altitude in more dense atmosphere. The energy consumption of that pump is an important consideration in the design of the aerobot. Release of some or all of the pressurized gas to ascend in altitude generally requires negligible energy consumption since a valve can be opened to simply vent the gas into the zero pressure balloon. The mechanical compression balloon typically works by pulling on a cable that connects the north and south poles of the balloon, or stack of interconnected balloons, thereby changing the volume. This requires an actuator to provide the pulling force, and that will consume a certain amount of energy. Expanding the balloon again is a simple matter of releasing the brake and allowing the internal pressure to unspool the cable, another operation that nominally requires very little energy. This power consumption disparity between ascent and descent means that these aerobots will typically ascend at a much faster rate than they descend.

Another characteristic shared by all three aerobot types is that the energy consumed by altitude changes scales with the amount of superpressure in the pressurized part of the vehicle. In the limit of zero superpressure, the aerobot will essentially be a zero pressure balloon that is neutrally stable in altitude. A defining feature of this neutral stability is that any perturbation will cause the vehicle to displace vertically without limit, which means that there will be effectively zero energy consumption to change altitude. In this context, the problem of a neutrally-stable vehicle is that Venus and Titan missions require keeping the balloon in a defined altitude range either to avoid hitting the surface (Titan), or avoid entering the unsurvivably hot lower atmosphere (Venus), or avoid bursting the balloon by ascending beyond the design altitude (both).

We therefore argue as a practical matter that it is necessary to have some amount of superpressure at least at the lower altitude bound so that the vehicle can arrest the downward motion caused by sustained vertical downwards winds or the setting sun. For pumped helium balloons the transfer (venting) of pressurized helium to the zero pressure balloon will increase the buoyancy to arrest the downwards motion. For air ballast balloons the venting of pressurized air will decrease the weight to arrest the downwards motions. For mechanical compression balloons, the pressurized helium will expand the balloon volume to create more buoyancy and arrest the downwards motion. In addition to acting as a pressurized reservoir of gas, the fact that some or all of the aerobot is a superpressure balloon will also provide an altitude-stabilizing function because such balloons are inherently stable in altitude due to being essentially constant volume structures.

Near the maximum altitude boundary it is possible to arrest undesirable vertically upwards motion by sufficiently rapid gas pumping (for PH and AB balloons) or cable pulling (MC balloon) to quickly change the aerobot's net buoyancy. However, electrical power and mass tend to be highly limited resources on any space mission and therefore it may not be possible to provide for the sufficiently rapid pumping or cable pulling in a practical design. If so, then once again there would be a need for some amount of superpressure in a certain volume to passively provide an altitude stabilizing function to keep the vehicle from ascending too high.

It turns out that the superpressure amount in all three types of balloons is not a free variable once it is specified for at least one altitude in a given design. In particular, superpressure cannot be raised near the altitude extrema to boost stability but dropped in intermediate altitudes to save power. The next subsection of the paper will present a derivation of underlying relationships that show non-zero superpressure across the entire range of altitudes; therefore, the zero-energy limit for altitude changes cannot be achieved in practice.

Variable Altitude Balloon Theory For Superpressure

For all analyses, we will assume the atmosphere acts as an ideal gas with constant molar composition. Accordingly, the atmospheric density ρ_a is given by:

$$\rho_a = \frac{P}{R_a T} \tag{1}$$

where P, T, and R_a are the atmospheric pressure, temperature, and atmospheric gas constant respectively. We will similarly assume that the helium or any alternate buoyancy gas also acts as an ideal gas.

We make the simplifying assumption in this analysis that the atmosphere gas and the buoyancy gas have the same temperature. This is a good assumption for flight under nighttime conditions but significant deviation would be expected with solar heating. These deviations are readily computed with numerical analysis for example point designs later in the paper, but no simple algebraic description has yet been found to match the non-solar heated cases described below.

By definition, the atmosphere and balloon gas pressures will be equal for a zero pressure balloon. Therefore, the volume of any zero pressure balloon is given by:

$$V_{zp} = \frac{n_{zp} R T}{P} \tag{2}$$

where n_{zp} is the number of moles of helium in the zero-pressure balloon, and R is the universal gas constant. The zero-pressure balloon's gross buoyancy (in kilograms) is the mass of the displaced air:

$$B_{zp} = \rho_a V_{zp} = \frac{P}{R_a T} \frac{n_{zp} R T}{P} = \frac{n_{zp} R}{R_a} \tag{3}$$

When at an equilibrium altitude, this gross buoyancy will be equal to the sum of the masses of the balloon, payload and helium. Note that under the assumption that the temperature inside and outside the balloon is the same a zero pressure balloon is only neutrally stable; the gross buoyancy is constant with altitude and *only* dependent on the amount of helium inside.

A superpressure balloon's volume is a constant value V_{sp}; therefore, the gross buoyancy is:

$$B_{sp} = \rho_a V_{sp} = \frac{P}{R_a T} V_{sp} \tag{4}$$

The volume V_{sp} of this type of balloon stays constant, but the buoyancy changes as the outside temperature T and pressure P changes.

We will now derive superpressure relations for each of the five types of variable altitude balloons.

Pumped Helium (PH) Balloon 1 – Balloon within Balloon

The PH balloon-within-a-balloon architecture consists of two separate gas volumes. The super-pressure volume is equal to that of the inner balloon, while the zero-pressure volume is equal to the outer volume minus the inner volume. In this framework, the PH balloon-within-a-balloon and PH tandem balloon are almost equivalent; the only difference is the geometry of the envelopes that contain the gas.

Bulk-gas expressions are agnostic to this geometry and therefore apply to both PH balloon types. Accordingly, the analysis in the next section holds for either system.

Pumped Helium (PH) Balloon 2 – Tandem Balloons

For a PH balloon, both the zero-pressure and the super-pressure volumes contribute buoyancy. Taking the two volumes together, we thereby obtain a total gross buoyancy:

$$B = B_{zp} + B_{sp} = \frac{n_{zp}R}{R_a} + \frac{P}{R_a T} V_{sp} \tag{5}$$

Let us now consider two different altitudes, where the pressures and temperatures are P_1 & P_2 and T_1 & T_2 respectively. The system mass does not change; therefore, we need to ensure that the buoyancy stays the same at both altitudes to ensure equilibrium:

$$B_1 = B_2 \tag{6}$$

$$\frac{n_{zp,1}R}{R_a} + \frac{P_1}{R_a T_1} V_{sp} = \frac{n_{zp,2}R}{R_a} + \frac{P_2}{R_a T_2} V_{sp} \tag{7}$$

Solving for the moles of helium transferred in/out of the zero-pressure balloon to keep a constant buoyancy, we obtain:

$$n_{zp,2} - n_{zp,1} = \left(\frac{P_1}{T_1} - \frac{P_2}{T_2}\right)\frac{V_{sp}}{R} \tag{8}$$

Next, we solve for the moles of helium inside the super-pressure balloon. Assuming the ideal gas law, we obtain:

$$n_{sp} = \frac{(P + \Delta P)V_{sp}}{RT} \tag{9}$$

where ΔP is amount of superpressure in the balloon above atmospheric pressure. Again applying this analysis at two different altitudes, we can solve for the helium transferred into or out of the super-pressure balloon:

$$n_{sp,1} - n_{sp,2} = \frac{(P_1 + \Delta P_1)V_{sp}}{RT_1} - \frac{(P_2 + \Delta P_2)V_{sp}}{RT_2} \tag{10}$$

Conserving mass, the helium transferred in/out of the zero-pressure balloon must the exact opposite of the helium transferred in/out of the super-pressure balloon. Accordingly:

$$n_{zp,2} - n_{zp,1} = n_{sp,1} - n_{sp,2} \tag{11}$$

Substituting Equations (8) and (10) into Equation (11), we can solve for the superpressure ΔP:

$$\left(\frac{P_1}{T_1} - \frac{P_2}{T_2}\right)\frac{V_{sp}}{R} = \frac{(P_1 + \Delta P_1)V_{sp}}{RT_1} - \frac{(P_2 + \Delta P_2)V_{sp}}{RT_2} \tag{12}$$

$$\frac{P_1}{T_1} - \frac{P_2}{T_2} = \frac{P_1 + \Delta P_1}{T_1} - \frac{P_2 + \Delta P_2}{T_2} \tag{13}$$

$$\frac{\Delta P_2}{T_2} = \frac{\Delta P_1}{T_1} \tag{14}$$

This shows that the superpressure is proportional to the absolute atmospheric temperature:

$$\Delta P \propto T \tag{15}$$

A planetary atmosphere generally shows a slowly changing temperature with altitude (the lapse rate) and therefore we would expect the superpressure of a PH aerobot also to show a slowly changing value with altitude.

Calling our constant of proportionality k_T, we now return to Eq. 9 to solve for its numerical value.

$$\Delta P = k_T T \tag{16}$$

$$n_{sp} = \frac{(P + k_T T)V_{sp}}{RT} = \frac{PV_{sp}}{RT} + \frac{k_T V_{sp}}{R} \tag{17}$$

$$k_T = \frac{R}{V_{sp}}\left(n_{sp} - \frac{PV_{sp}}{RT}\right) \tag{18}$$

Finally, k_T can be simplified to:

$$k_T = \frac{R}{V_{sp}}\left(n_{sp} - n_{sp}|_{\Delta P=0}\right) \tag{19}$$

where $n_{sp}|_{\Delta P=0}$ is the baseline number of moles of helium in the superpressure balloon if it were vented all the way to the point of no super-pressure and hence become a zero pressure balloon of volume V_{sp}. As we would expect, k_T is dependent on the number of moles of buoyancy gas that create the non-zero superpressure, namely the amount of excess gas beyond that needed to exactly fill the volume and yet remain a zero pressure balloon. As k_T is constant with altitude, the amount of excess gas is also constant with altitude.

Air Ballast (AB) Balloon 1 – Tandem Balloons

On an AB balloon, we can use similar arguments to determine how the superpressure scales with altitude. The gross buoyancy relation of a tandem AB balloon is equivalent to the PH balloon:

$$B = B_{zp} + B_{sp} = \frac{n_{zp}R}{R_a} + \frac{P}{R_a T} V_{sp} \tag{20}$$

However, we now note that unlike the PH balloon, the air pump changes the mass of the AB balloon which must be accommodated by an equal change in the gross buoyancy.

$$B_{zp} + B_{sp} = m_{sp} + M \tag{21}$$

where m_{sp} is the *variable* air mass in the superpressure balloon, and M is the mass of the rest of the system. Evaluating Equation 21 at two separate altitudes (1 and 2) and noting that B_{zp} and M stay constant regardless of altitude for this balloon:

$$B_{sp,1} - m_{sp,1} = M - B_{zp} = B_{sp,2} - m_{sp,2} \tag{22}$$

$$\frac{P_1}{R_a T_1} V_{sp} - \frac{(P_1 + \Delta P_1)}{R_a T_1} V_{sp} = \frac{P_2}{R_a T_2} V_{sp} - \frac{(P_2 + \Delta P_2)}{R_a T_2} V_{sp} \tag{23}$$

$$\frac{\Delta P_2}{T_2} = \frac{\Delta P_1}{T_1} \tag{24}$$

$$\Delta P \propto T \tag{25}$$

This is the same superpressure relationship derived for the PH balloon. Again calling this constant of proportionality k_T, i.e. $\Delta P = k_T T$, we can return to the ideal gas law to determine a closed-form expression for it:

$$n_{sp} = \frac{(P + k_T T) V_{sp}}{RT} \tag{26}$$

$$k_T = \frac{R}{V_{sp}} \left(n_{sp} - n_{sp}|_{\Delta P = 0} \right) \tag{27}$$

This is the same expression as the PH balloon, only now we are counting moles of air ballast, rather than moles of helium, in the super-pressure balloon.

Air Ballast (AB) Balloon 2 – Ballonet

The buoyancy for the ballonet air-ballast balloon acts as one single super-pressure balloon:

$$B = \rho_a V = \frac{P}{R_a T} V \tag{28}$$

The mass of this balloon changes as air is pumped into the ballonet. Accordingly,

$$\frac{P}{R_a T} V = B = m_a + m_{he} + M \tag{29}$$

where m_a is the mass of air in the ballonet, m_{he} is the mass of helium, and M is the mass of everything else. Evaluating Equation (29) at two different altitudes, we note that m_{he} and M are constant:

$$\frac{P_1}{R_a T_1} - m_{a,1} = m_{he} + M = \frac{P_2}{R_a T_2} - m_{a,2} \tag{30}$$

$$\frac{P_1}{R_a T_1} - \frac{P_2}{R_a T_2} = m_{a,1} - m_{a,2} \tag{31}$$

The mass transfer of air into the ballonet adds to the total number of moles *n* of gas in the two-compartment balloon.

$$m_{a,1} - m_{a,2} = \frac{R}{R_a}(n_1 - n_2) \tag{32}$$

The total number of moles in the balloon can now be expressed using the ideal gas law, which relates the super-pressure to the balloon volume:

$$n = \frac{(P + \Delta P)V}{RT} \tag{33}$$

Substituting back into Equation (32) simplifies to our proportionality expression:

$$\frac{P_1}{R_a T_1} - \frac{P_2}{R_a T_2} = \frac{R}{R_a}\left(\frac{(P_1 + \Delta P_1)V}{RT_1} - \frac{(P_2 + \Delta P_2)V}{RT_2}\right) \tag{34}$$

$$\frac{\Delta P_2}{T_2} = \frac{\Delta P_1}{T_1} \tag{35}$$

$$\Delta P \propto T \tag{36}$$

Again, solving for this proportionality constant k_T in $\Delta P = k_T T$ gives the now familiar expression:

$$k_T = \frac{R}{V}(n - n|_{\Delta P = 0}) \tag{37}$$

Mechanical Compression Balloon

Finally, we address the MC balloon. The buoyancy expression of the MC balloon similar to that of a standard super-pressure balloon, Equation (4):

$$B = \rho_a V = \frac{P}{R_a T}\frac{nRT}{P + \Delta P} \tag{38}$$

Applying this buoyancy to two altitudes (1 and 2) we can determine a relation for the super-pressure. Note that for the MC balloon, both the buoyancy and helium mass do not change, but the volume does.

$$B_1 = B_2 \tag{39}$$

$$\frac{P_1}{R_a}\frac{nR}{P_1 + \Delta P_1} = \frac{P_2}{R_a}\frac{nR}{P_2 + \Delta P_2} \tag{40}$$

$$\frac{P_1}{P_1 + \Delta P_1} = \frac{P_2}{P_2 + \Delta P_2} \tag{41}$$

Which simplifies to the proportionality:

$$\Delta P \propto P \tag{42}$$

Note that this behavior is distinctly different from the PH or AB balloons, whose super-pressure is proportional to the atmospheric temperature instead. Calling the constant of proportionality k_P, i.e. $\Delta P = k_P P$, we can solve for it by noting the ideal gas law:

$$(P + k_P P)V = nRT \tag{43}$$

$$k_P = \frac{RT}{PV} n - 1 \tag{44}$$

$$k_P = \frac{n}{n|_{\Delta P=0}} - 1 \tag{45}$$

Again, $n|_{\Delta P=0}$ is the number of moles of helium remaining if the MC balloon was vented until the superpressure equaled zero.

It can be seen in the preceding derivations that the five types of variable altitude balloons divide into two groups of superpressure behavior: the PH and AB balloons all show a ΔP ~ T behavior, while the MC balloon shows a ΔP ~ P behavior. Given that atmospheric pressure tends to change with altitude more quickly than temperature, this suggests we will experience larger ΔP variations with the MC balloon when solar heating is ignored. In all cases, however, the ΔP versus altitude behavior is prescribed by these scaling laws and is not a free variable in the aerobot design.

Work and Energy Calculations

For non-zero superpressure, work must be done to compress the gas when moving from a higher to a lower altitude. The reverse does not require work to be done since the compressed gas can simply be vented from its pressurized state. The work done from the higher to lower altitude can be computed from basic fluid mechanics and thermodynamics. There are two cases:

1. Pump work based on the flow of helium or air into a pressurized reservoir (PH and AB aerobots).
2. Cable pulling to perform pressure-volume (PdV) work on a fixed mass of helium (MC).

The work done to pump a gas under steady-state conditions is given by the mass flow rate times the change in enthalpy:

$$\dot{W}_{pump} = \dot{m}_{gas}\,(h_{out} - h_{in}) \tag{46}$$

where $\dot{W}_{pump}$ is the work done by the pump, $\dot{m}_{gas}$ is the mass flow rate of the gas through the pump, h_{out} is the enthalpy of the gas at the pump outlet, and h_{in} is the enthalpy of the gas at the pump inlet. We can rewrite this equation in terms of temperature and pressure by using the standard ideal gas isentropic relationships:

$$h = C_P T \tag{47}$$

$$\left(\frac{T_{out}}{T_{in}}\right) = \left(\frac{P_{out}}{P_{in}}\right)^{\frac{\gamma-1}{\gamma}} \tag{48}$$

where C_P is the specific heat capacity, T is the temperature, P is the pressure and γ is the ratio of specific heats. Use of this relationship means that from this point on we are computing the ideal work for a reversible process.

Substituting Equations (47) and (48) into (46) yields:

$$\dot{W}_{pump} = \dot{m}_{gas} C_P T_{in} \left[\left(\frac{P_{out}}{P_{in}}\right)^{\frac{\gamma-1}{\gamma}} - 1\right] \tag{49}$$

This can be integrated in time to compute the total ideal pump energy consumption:

$$\Delta E_{pump} = \int_{t_i}^{t_f} \dot{W}_{pump}\, dt = \int_{t_i}^{t_f} \dot{m}_{gas} C_P T_{in} \left[\left(\frac{P_{out}}{P_{in}}\right)^{\frac{\gamma-1}{\gamma}} - 1\right] dt \tag{50}$$

where t_f and t_i are the final and initial times of the pumping interval. Noting that $\dot{m}_{gas} = \frac{dm_{gas}}{dt}$, the integral can be re-written in terms of mass change rather than time change:

$$\Delta E_{pump} = \int_{m_i}^{m_f} C_P T_{in} \left[\left(\frac{P_{out}}{P_{in}}\right)^{\frac{\gamma-1}{\gamma}} - 1\right] dm_{gas} \tag{51}$$

where m_f and m_i are the final and initial mass of gas in the pressurized reservoir. This equation shows that the ideal pump energy to move from one altitude to another is time independent. In practice, this integral can be evaluated knowing the helium gas mass as a function of altitude

calculated from a series of quasi-static equilibrium points. Note also that the energy dependence on aerobot superpressure can be made explicit by substituting

$$P_{out} = P_{in} + \Delta P \tag{52}$$

where ΔP is the superpressure.

For the mechanical compression balloon, the actuator plus cable assembly does work equal to the applied force times distance on the cable, which must be equal to the PdV work done on the gas inside the balloon:

$$\Delta E_{MC} = F * d = -\int_{V_i}^{V_f} \Delta P \, dV \tag{53}$$

where F is the cable force, d is the distance moved by the cable, ΔP is the gas superpressure, V is the gas volume, v_i is the initial gas volume and v_f is the final gas volume. Note that the winch only does work on the balloon gas proportional to the excess pressure (superpressure) above ambient.

Venus Point Designs

We present data in this section on Venus point designs for each type of light gas variable altitude aerobot, including comparisons of vehicle mass and ideal work done (energy consumption) for changing altitude. This is not an exhaustive trade study of the design space but does present feasible designs that can be compared to draw conclusions about the performance differences between the different platforms.

These point designs are based on a common mission scenario in which the aerobot floats at high altitude in the Venusian clouds at temperatures compatible with standard spacecraft avionics and instruments. In each case, the aerobot has a not-to-exceed 100 kg payload module suspended below the balloon that includes everything needed for the mission including science instruments, avionics, structure, telecommunications and power system. We specify that the aerobot is able to control its altitude between a 52 and 60 km altitude, a range that spans much of the cloud layer of Venus and is of high importance for investigating the cloud aerosols, sulfur-based chemistry, winds and solar heating. Given the results from the 1985 VEGA balloon flights at Venus[8] we assume a worst case sustained vertical wind of 3 m/s that the aerobot must tolerate at the upper and lower bounds of the 52 to 60 km range. The point design analyses performed here do not include detailed solar heating calculations of the gas inside the balloon but instead use a simplifying assumption that the helium gas would increase in temperature by 36 K at 60 km, linearly decreasing by 2 K/km so that the temperature increase would be only 20 K at 52 km. This assumption captures the gross behavior that the clouds will attenuate the solar flux as one decreases in altitude; however, we expect the actual temperatures will vary from these approximate values once the full heat transfer analysis with real balloon materials is included.

The analyses use standard Venus atmosphere properties as listed in Table 1. We assume a gas mixture of 97% CO_2 and 3% N_2. Helium is the buoyancy gas inside the balloon. Helium and the Venus atmosphere are treated as perfect gases.

The presence of sulfuric acid aerosols in the Venus atmosphere across this altitude range requires the use of non-standard balloons materials. Prior development work of prototype Venus

Table 1: Venus Atmosphere Properties

Altitude (km)	Temperature (K)	Pressure (Pa)	Density (kg/m^3)
62	254.5	16,588	0.3411
60	262.8	23,571	0.4694
59	268.7	27,972	0.5448
58	275.2	33,071	0.6289
57	282.5	38,930	0.7212
56	291.8	45,626	0.8183
55	302.3	53,183	0.9207
54	312.8	61,682	1.0320
53	323.0	71,162	1.1530
52	333.3	81,774	1.2840

superpressure balloons resulted in laminate materials that used Teflon as the acid barrier, Vectran fabric as the strength element and metallization to reflect sunlight and thereby minimize solar heating.[9,10] We adopt that basic approach for the point designs in this paper, although we recognize that tendon-reinforced (pumpkin) balloon designs may offer mass advantages for superpressure balloons compared to this laminated material. Note that there are four types of laminate materials needed to compute point designs for the five aerobot types:

1. Zero pressure balloon, no Vectran required, but with Teflon to resist the acid.
2. Superpressure balloon inside the zero pressure balloon, no Teflon required.
3. Superpressure balloon exposed to acid on the outside surface, requires the full laminate from prior work scaled to the estimated superpressure loads.
4. Superpressure balloon exposed to acid on both the external and internal surfaces, requires the full laminate plus Teflon on the inside surface as well.

Estimated areal densities (mass per unit area) for these materials are listed in the results summary presented as Table 2. A 30% construction factor is added to each areal density to account for seams and end cap reinforcements, and then another 20% is added as a design margin. The balloon areal densities are derived from the materials listed in References 9 and 10 with the amount of Vectran adjusted to provide a structural safety factor of approximately 2 compared to the stress resulting from the superpressure and size of balloon. For the single-balloon AB case, we assume a hemispherical dividing membrane.

Point designs for each Venus aerobot are based on solving the set of algebraic equations that determine the conditions at each equilibrium altitude. The equilibrium altitude is defined by weight equals buoyancy force. In practice, the calculation iterates on the balloon size(s) to yield feasible solutions across the entire altitude range. We model all of the balloons as spheres, noting that for the MC concept in particular that practical implementation may require a stack of balloons to achieve a sufficient compression ratio over a large altitude range. A driving design feature is that all options maintain a small 1000 Pa superpressure margin to avoid loss of control authority under the worst case flight conditions of minimum altitude, no solar heating, and a downwards sustained wind of 3 m/s. This constraint sets the amount of excess helium required to compensate for the

worse case disturbance, given the balloon size and specified payload mass. In turn, this leads to solving the set of equations where the dependent variable is different in each case:

- For the pumped helium aerobot, the variable is the relative amounts of helium in the zero and superpressure balloons.
- For the air ballast aerobot, the variable is the amount of air in the superpressure balloon.
- For the mechanical compression aerobot, the variable is the balloon volume.

For the vertical wind calculations, we assume a drag coefficient of 0.5 for the aerobot. Single balloon concepts use the cross-sectional area of the balloon modeled as a sphere corresponding to the given volume. For tandem balloon concepts we modify the cross-sectional reference area to be the main zero pressure balloon area modeled as a sphere and one-half the secondary superpressure balloon area modeled as a sphere. This latter assumption presumes some drag reduction resulting from one balloon being in the wake of the other balloon.

Table 2 presents the results for all point designs with a 100 kg payload module for the 52 to 60 km altitude range. The ideal energy values are computed by numerical integration of the formulas in Equations 51 or 53 as appropriate.

Carrying a 100 kg payload requires a helium balloon over 10 meters in diameter at this altitude range at Venus for all five concepts. Given that pressure-loaded balloon material is much heavier than zero pressure material, the size of the superpressure balloon tends to dominate the overall aerobot mass; therefore, the concepts that require the largest superpressure balloons, namely the air ballast and mechanical compression balloons, are also the most massive. The helium mass clearly scales with overall floating mass as would be expected. Setting the smaller balloon to be roughly half the diameter of the larger balloon in the two balloon concepts also seems to yield the lowest mass designs for this scenario.

The predicted $\Delta P \sim T$ behavior (Equations 15, 25, 36) for the PH and AB concepts is clearly shown in the superpressure values for nominal night conditions at 52 and 60 km altitude. In each case the superpressure ratio equals 1.27 in accord with the atmospheric temperature ratio of 333.3 K / 262.8 K = 1.27. Similarly, the MC concept shows the $\Delta P \sim P$ behavior (Eq. 42) with the superpressure ratio equal to the atmospheric pressure ratio of 81,774 Pa / 23,571 Pa = 3.47.

There are important differences between the concepts in terms of maximum superpressure and altitude stability as shown by the results in Table 2. The PH and two-balloon AB aerobots have the smallest superpressure balloon envelopes, require the largest superpressures and experience the largest excursions above the nominal 60 km maximum altitude. Note that this reflects a design assumption that these aerobots must passively resist the vertically upwards displacement due to perturbing wind since pumping speeds are expected to be low given the likely constraints on pump size and electrical power. Smaller superpressure balloons in an updraft will therefore displace and pressurize more until equilibrium is re-established at the higher altitude. The single large AB aerobot is very stable in altitude and experiences a much reduced superpressure increase. This lower superpressure explains why the single AB aerobot requires a balloon material with less mass per unit area than the two-balloon AB aerobot.

The MC aerobot obeys a different superpressure relationship with no solar heating than the other concepts, namely $\Delta P \sim P$ instead of $\Delta P \sim T$, and this manifests itself in some unique results as shown in Table 2. Note that the ambient pressure varies by a factor of 3.47 across the 60 to 52 km altitude range in contrast to the ambient absolute temperature that varies only be a factor of 1.27. The MC aerobot therefore experiences its highest superpressure at the lowest altitude where the ambient pressure is highest, even at night. The single balloon AB concept also shares this property, in contrast to the other concepts that have the highest superpressure at the maximum

Table 2: Summary of Venus Aerobot Point Design Results for 52 to 60 km Range

	PH (balloon in balloon)	PH (two balloon)	AB (two balloon)	AB (one balloon)	MC (one balloon)
Maximum nominal altitude (km)	60	60	60	60	60
Minimum nominal altitude (km)	52	52	52	52	52
Zero-P (ZP) balloon diameter	10.6	10.4	12.6	N/A	N/A
Superpressure (SP) balloon diameter	5.30	5.2	6.93	11.8	10.5
ZP balloon areal density (g/m^2)	120	120	120	120	N/A
SP balloon areal density (g/m^2)	170	270	330	285	270
Nominal Superpressure (Pa) [Night, High Altitude, No wind]	9,100	9,600	7,100	2,900	2,800
Nominal Superpressure (Pa) [Night, Low Altitude, No wind]	11,500	12,200	9,000	3,600	9,800
Maximum superpressure (Pa)	32,800	36,300	31,300	8,700	10,800
Maximum Superpressure Condition **D**ay/**N**ight, **H**igh/**L**ow Altitude, **U**pdraft/**N**o wind/**D**owndraft	D,H,U	D,H,U	D,H,U	D,L,N	D,L,N
Minimum superpressure (Pa) [Night, Low altitude, Downdraft]	1,000	1,000	1,000	1,000	1,000
Total helium mass	20.6	21.6	29.9	38.9	26.8
Total balloon mass	89.5	99.4	171.0	235.4	145.9
Total aerobot mass (w/o helium)	189.5	199.4	271.0	335.4	245.9
Maximum perturbed altitude (km)	62.0	62.1	61.8	60.3	60.3
Daylight ideal energy required to go from max to min altitude (J)	1,270,000	1,264,000	2,843,000	6,282,000	2,660,000
Nighttime ideal energy required to go from max to min altitude (J)	712,000	732,000	1,242,000	2,591,000	1,061,000

altitude with solar heating and vertical wind displacements. The large MC balloon size provides excellent altitude stability to wind displacements but the existence of relatively high superpressure at the lowest altitudes drives up the energy cost for changing altitude.

The MC aerobot falls in the middle of the range of energy costs, as does the two balloon AB aerobot. The PH aerobot requires the least energy and there is no appreciable difference between the one- and two-balloon options. The single AB aerobot requires by far the most energy to change altitude. These energy results appear to mirror the expected behavior that the least stable aerobots require the least energy to decrease altitude. In the limit of neutrally stable zero pressure balloons, as we noted above, no energy is required to change altitude.

Two energy values are provided for each concept in Table 2, one for a solar-heated aerobot and one without. Non solar-heated aerobots always have lower energy requirements given the lower superpressures; however, the PH aerobots show a relatively small change (80% increase in daylight) while the AB aerobots show a much larger change (270% increase in daylight). This difference is presumably due to the larger mass of ingested air inside the AB aerobots that heats

up and must be compressed to reduce altitude. The MC aerobot behaves like the PH aerobots in terms of energy consumption, probably because all of these concepts do work only on the mass of helium buoyancy gas and not on any additional ingested atmosphere.

We explored a second mission scenario for Venus in which the maximum altitude was increased from 60 to 62 km. This was done primarily to understand the sensitivity of the different aerobot designs to accommodating a larger density difference between the maximum and minimum altitudes. The results are shown in Table 3. Most notable in this table was the inability to generate feasible designs for either air ballast concept. The growth in balloon size with the higher altitude combined with an attendant increase in balloon material mass per unit area to provide increased tensile strength for the larger sizes resulted in a runaway vehicle mass that could not be balanced by buoyancy. The pumped helium and mechanical compression concepts all show modest increases in balloon size, helium mass, ideal pump or compression energy to change altitude, but all yielded reasonable design solutions.

Titan Point Designs

In addition to conducting *in situ* atmospheric investigations, an aerobot at Titan can enable global-scale aerial reconnaissance of the surface when flying in the lowest part of the atmosphere. Aerobots that approach the surface, or that deploy a separate daughtercraft, can also do surface sample acquisition and thereby enable composition measurements at widely separated and diverse terrain types. We choose such a mission scenario to compare the different types of aerobots in this study with the following criteria and assumptions:

- Altitude range from 1 to 11 km above the surface.
- 200 kg payload module mass carried by the balloon.
- Maximum heating of the balloon gas of 1 K during daytime.
- Maximum sustained vertical winds of 0.5 m/s.

The payload mass for Titan is chosen to be double that for the Venus scenario to incorporate a number of extra elements including: a radioisotope thermal generator (RTG) for electrical power generation, a system for performing surface sample acquisition and analysis, and additional thermal control and telecommunications mass to accommodate the cryogenic Titan environment and larger distance to Earth.

The analyses use standard Titan atmosphere properties listed in Table 4. The temperature and pressure data in Table 4 are measurements taken by the Huygens probe[11], and the density is a derived quantity using the ideal gas law and a 5% CH_4, 95% N_2 average atmosphere composition. Note the key differences between the Titan atmosphere and that used for the Venus aerobot calculations, namely the cryogenically cold temperature, the mostly nitrogen atmosphere instead of carbon dioxide, and the much reduced solar heating and winds.

Prior work on Titan blimp concepts included development of cryogenically compatible polyester film and fabric balloon materials.[12,13] We adopt the lighter weight 75 g/m^2 material for the zero pressure balloons in these point designs. It will be shown that the Titan superpressure balloons in this study experience higher superpressures and hence require more tensile strength than any material developed in the earlier Titan blimp work; therefore, we approximately scaled the prior materials into the range of 120 to 160 g/m^2 as required. Both the zero pressure and superpressure balloon materials are significantly lighter than those used at Venus, partly because

Table 3: Summary of Venus Aerobot Point Design Results for 52 to 62 km Range

	PH (balloon in balloon)	PH (two balloon)	AB (two balloon)	AB (one balloon)	MC (one balloon)
Maximum nominal altitude (km)	62	62	No feasible design	No feasible design	62
Minimum nominal altitude (km)	52	52			52
Zero-P (ZP) balloon diameter	11.6	12.0			N/A
Superpressure (SP) balloon diameter	5.80	6.0			12.5
ZP balloon areal density (g/m^2)	120	120			N/A
SP balloon areal density (g/m^2)	170	270			270
Nominal Superpressure (Pa) [Night, **High Altitude,** No wind]	6,800	6,800			2,200
Nominal Superpressure (Pa) [Night, **Low Altitude**, No wind]	8,900	8,900			10,800
Maximum superpressure (Pa)	28,100	28,200			10,200
Maximum Superpressure Condition **D**aylight/**N**ight, **H**igh/**L**ow, **U**pdraft/**N**o wind/**D**owndraft	D,H,U	D,H,U			D,L,N
Minimum superpressure (Pa) [Night, Low altitude, Downdraft]	1,000	1,000			1,000
Total helium mass	22.4	25.1			33.2
Total balloon mass	107.2	132.3			206.8
Total aerobot mass (w/o helium)	207.2	232.3			306.8
Maximum perturbed altitude (km)	63.6	63.5			62.2
Daylight energy required max to min altitude (J)	1,857,000	2,062,000			4,349,000
Nighttime energy required max to min altitude (J)	954,000	1,056,000			1,528,000

there is no need for Teflon to protect against corrosive acids and partly because the Titan scenario requires smaller balloon sizes and smaller superpressure levels.

The solution methodology for Titan point designs is the same as described above for Venus. The results are summarized in Table 5 for all five aerobot concepts.

The Titan results show a number of key differences with the Venus results. Most noticeably, the Titan balloons are much smaller than the Venus balloons, a benefit of flying in a much denser atmosphere. In addition, the density difference between the lowest and highest altitude is smaller at Titan, with a density ratio of only 1.5, compared to a ratio of 2.7 or 3.8 at Venus depending on whether the maximum altitude is 60 or 62 km. This smaller density ratio leads to superpressure balloon volumes at Titan being relatively larger compared to the zero pressure balloon volumes. The superpressure balloon volume is in fact slightly larger than the zero pressure balloon in this point design for the two balloon pumped helium concept. Another key difference is that the Titan aerobot maximum superpressure is generally much smaller than for Venus aerobots, with a range

Table 4: Titan Atmosphere Properties

Altitude (km)	Temperature (K)	Pressure (Pa)	Density (kg/m^3)
13.8	81.4	72,490	2.935
11.3	83.2	82,740	3.277
9.5	84.4	90,940	3.551
8.3	85.4	96,990	3.743
6.7	86.8	105,140	3.992
5.5	87.8	111,840	4.198
4.5	88.8	117,830	4.373
3.2	90.0	125,720	4.604
2.0	91.2	133,370	4.820
1.1	92.3	139,380	4.977
0.3	93.1	144,670	5.121
0	93.7	146,700	5.160

of 4,400 to 7,600 Pa compared to 8,700 to 36,300 Pa. This results from a combination of much smaller solar heating plus smaller atmospheric temperature and pressure ratios between the maximum and minimum altitude. In turn, the smaller superpressures and smaller balloons lead to much smaller balloon masses for Titan as compared to Venus. The data in Table 5 shows that the balloon mass is roughly 10% of the payload mass for all concepts, as compared to Venus where the balloon mass was roughly equal to or much more than the payload mass depending on the concept. As a result, the total floating mass for Titan aerobots is close to the best Venus concepts despite having double the payload mass.

All Titan designs require almost the same helium mass in a narrow range of 38.4 to 40.1 kg. These values are substantially higher than the best Venus design (20.6 kg for the PH aerobot) and reflects the reduced buoyancy efficiency in the mostly nitrogen atmosphere of Titan (density ratio of ~28/4 = 7) compared to the mostly carbon dioxide atmosphere of Venus (density ratio of ~44/4 = 11). All of the Titan concepts except the two-balloon PH option show very little excursion (~ 0.3 km) above the nominal 11 km maximum altitude, with the two balloon PH option at a modest 0.7 km. Although one might expect that the low gravity would result in large altitude displacements, this is compensated by the low solar heating and assumed low vertical wind that drive the perturbation.

The final key difference between the Titan and Venus aerobot results is the much reduced energy required to decrease altitude at Titan. All of the Titan aerobots require more than an order of magnitude less energy to change altitude as a result of the much lower superpressures and reduced pumping or compression requirements due to the smaller density ratios between the maximum and minimum altitude. Although there are some energy differences between the Titan concepts, the values are so small that energy may not be a significant discriminator between the concepts. This mirrors the conclusion for overall system mass comparisons in that while the MC and PH aerobots are the lowest mass, the quantitative difference is so small that it is probably not a strong discriminator in choosing between the concepts.

Table 5: Summary of Titan Aerobot Point Design Results for 1 to 11 km Altitude Range

	PH (balloon in balloon)	PH (two balloon)	AB (two balloon)	AB (one balloon)	MC (one balloon)
Maximum nominal altitude (km)	11	11	11	11	11
Minimum nominal altitude (km)	1	1	1	1	1
Zero-P (ZP) balloon diameter	5.6	4.2	5.6	N/A	N/A
Superpressure (SP) balloon diameter	4.5	4.4	5.0	5.5	5.5
ZP balloon areal density (g/m^2)	75	75	75	75	N/A
SP balloon areal density (g/m^2)	140	140	160	120	140
Nominal Superpressure (Pa) [Night, **High Altitude,** No wind]	3,100	2,700	3,300	2,400	1,900
Nominal Superpressure (Pa) [Night, **Low Altitude**, No wind]	3,500	3,100	3,700	2,700	3,200
Maximum superpressure (Pa)	6,700	6,200	7,600	4,400	4,600
Maximum Superpressure Condition **D**aylight/**N**ight, **H**igh/**L**ow, **U**pdraft/**N**o wind/**D**owndraft	D,H,U	D,H,U	D,H,U	D,H,U	D,L,N
Minimum superpressure (Pa) [Night, Low altitude, Downdraft]	1,000	1,000	1,000	1,000	1,000
Total helium mass	39.5	38.4	41.0	39.6	38.7
Total balloon mass	25.3	19.8	31.1	23.3	20.8
Total aerobot mass (w/o helium)	225.3	219.8	231.1	223.3	220.8
Maximum perturbed altitude (km)	11.7	11.3	11.3	11.2	11.2
Daylight energy required max to min altitude (J)	93,600	82,800	136,300	113,700	93,900
Nighttime energy required max to min altitude (J)	62,000	52,400	78,500	75,100	61,100

Simulation Results

The point design calculations described above are based on simplified spreadsheet and Matlab-level tools that compute neutral buoyancy points with simplifying assumptions. The next level of analysis sophistication requires a high fidelity tool that computes the dynamics and thermodynamics in a full physics-based simulation. We have developed such a dynamics-based simulation model for variable altitude balloons using the Dynamics Simulator for Entry, Descent and Surface Landing (DSENDS) tool. DSENDS is a multi-mission flight dynamics modeling and simulation tool developed by the Dynamics and Real Time Simulation (DARTS) lab at JPL[14]. DSENDS is one of a family of simulation environments that build on the common Dshell framework. In addition to the DSENDS environment, the Rover Analysis, Modeling and Simulation (ROAMS) and RoboDarts simulation environments provide functionality tailored to vehicle dynamics and robotics applications, respectively. The underlying Dshell framework

provides core functionality for building complex multibody dynamics models and setting up, deploying and interacting with simulations. For speed, Dshell and DSENDS are written in C++ and provide a core set of models and reusable components. To support rapid simulation throughput and extensibility via third-party libraries, simulations are set up and deployed via a scripted Python interface. Refer to Ref. 14 for additional information.

DSENDS has been used to support a variety of NASA missions including Mars Phoenix, Mars Science Lab, the Insight Lander, and the Low Density Supersonic Decelerator (LDSD). Additionally, the software has been used to support the International Space Station (ISS), the Space Launch System (SLS) and future flight missions through a collaboration with Johnson Space Center. DSENDS provides sophisticated gravitational, aerodynamic and atmospheric models to support entry, descent and landing applications and has successfully been used to model balloons and parachutes to support the LDSD mission[14] and others. Refer to Ref. 15 for additional information.

Augmented Single Balloon Model

The primary governing equation for a one-dimensional DSENDS balloon model considering mass and virtual mass effects, gravitational, buoyancy and drag forces is:

$$(m_{tot} + C_m \rho_a V)\frac{d^2 z}{dt^2} = g\rho_a V - g m_{tot} - \frac{1}{2}\rho_a C_D \frac{dz}{dt}\left|\frac{dz}{dt}\right| A \tag{54}$$

where m_{tot} is the total system mass, C_m is the virtual mass coefficient, ρ_a is the atmospheric density, V is the balloon volume, g is the acceleration due to gravity, A is the cross-sectional area of the balloon and $\frac{dz}{dt}$ represents the vertical velocity. The quantity $(m_{tot} + C_m \rho_a V)$ represents the contribution due to mass and virtual mass effects, $g\rho_a V$ represents buoyancy forces, $g m_{tot}$ represents gravitational forces, and the quantity $\frac{1}{2}\rho_a C_D \frac{dz}{dt}|\frac{dz}{dt}|\, A$ represents aerodynamic drag force.

To support this effort, the standard DSENDS balloon buoyancy model above was augmented with a thermodynamic model and gas venting, which were first proposed by Carlson and Horne[16]. The thermodynamic model makes the simplifying assumption that the gas and film temperatures are spatially averaged values (i.e. temperature is uniform across the gas and film). Additionally, the atmosphere and balloon lifting gases are treated as ideal gases. The heat balance for balloon film is given as:

$$\dot{q}_f = m_f c_f \frac{dT_f}{dt} \tag{55}$$

where $\dot{q}_f$represents the net heat flux to the balloon film, $m_f$is the balloon film mass, $c_f$is the specific heat of the balloon film and $\frac{dT_f}{dt}$ represents the rate of change of film temperature with respect to time.

The heat balance for the balloon lifting gas is:

$$m_g c_{pg} \frac{dT_g}{dt} = \dot{q}_g - \frac{g M_a m_g T_g}{T_a M_g}\frac{dz}{dt} \tag{56}$$

where m_g represents the balloon gas mass, c_{pg} is the specific heat of the balloon gas, T_g is the balloon gas temperature, T_a is the temperature of the atmosphere, $\dot{q}_g$ represents the net heat flux to the balloon gas, M_a is the molecular weight of the atmosphere, and M_g is the molecular weight of the balloon gas.

The mass balance for the lifting gas is:

$$\frac{dm_g}{dt} = \frac{\rho_g M_g}{RT_g} \dot{E}_g - \dot{E}_v \tag{57}$$

where $\rho_g$is the density of the balloon gas, R is the universal gas constant and $\dot{E}_g$ and $\dot{E}_v$ are the balloon gas volume flow rates for expelling gas and valving respectively.

Additionally, the heat flux to the balloon film is a function of conductive, radiative and convective heat transfer, and is given as:

$$\dot{q}_f = [G\alpha_{weff}\left(\frac{1}{4}+\frac{1}{2}r_e\right) + \epsilon_{int}\sigma\left(T_g^4 - T_f^4\right) + CH_{gf}\left(T_g - T_f\right) + CH_{fa}\left(T_a - T_f\right) - \epsilon_{weff}\sigma T_f^4 + \epsilon_{weff}\sigma T_{BB}^4]S \tag{58}$$

where G is the solar constant, α_{weff} is the effective solar absorptivity of the balloon film, $r_e$is planet's reflectivity, $\epsilon_{int}$is the effective interchange IR emissivity, σ is the Stefan Boltzmann constant, CH_{gf} is the convective heat transfer coefficient between balloon film and gas, CH_{fa} is the convective heat transfer coefficient between balloon gas and film, T_{BB} is the black ball temperature and S is the balloon surface area. Likewise, the heat flux to the balloon gas is:

$$\dot{q}_g = \left[G\alpha_{geff}(1+r_e) - \epsilon_{int}\sigma\left(T_g^4 - T_f^4\right) - CH_{gf}\left(T_g - T_f\right) - \epsilon_{geff}\sigma T_f^4 + \epsilon_{geff}\sigma T_{BB}^4\right]S \tag{59}$$

where ϵ_{geff}represents the effective IR emissivity of the balloon gas. Refer to [16] for additional implementation details.

The above governing equations were written in C++ and embedded into a DSENDS balloon assembly. To validate the updated model, a single balloon from the Carlson and Horne paper was configured and deployed using the DSENDS Python interface. Atmospheric temperatures, pressures and gas properties were encoded in look-up tables and obtained using spline interpolation. The governing equations were numerically integrated using a variable rate, variable order implicit integrator based on the Adams-Moulton formula[17]. Overall excellent correspondence to the Carlson and Horne theory and flight data was found, lending confidence to the numerical implementation for the single balloon model.

Tandem Balloon Model

We have performed some initial simulations of the Venus Pumped Helium (PH) two-balloon configuration using a two-assembly version of the DSENDS model. To support exchange of gas between the two balloons via a pump, the two balloon models were configured to interface with one-another during simulation run-time via a message passing interface. Venus atmospheric temperatures, pressures and gas properties were encoded in a look-up table and were made accessible to both balloon models during the simulation. The balloon geometric and mass

properties for the PH (two balloon) configuration are the same as listed in Table 2. A schematic of the balloon model for this simulation is shown in Figure 2.

The atmospheric gas properties were obtained with the assumption that the Venus atmosphere is 97% CO_2 and 3% N_2. Additional gravitational parameters are summarized in Table 6.

Table 6: Venus Gravitational Parameters

Description	Value
Mass (kg)	4.8675e24
Equatorial radius (km)	6051.8
Mean density (kg/m^3)	5243

Two scenarios were simulated with a preliminary version of this tandem balloon model for Venus. Both scenarios are at night. In the first simulation, we compute the ascent of the PH tandem balloon system from 52 km up to 60 km. This is shown in Figure 3. The transfer (pumping) of helium from the superpressure reservoir to the main zero pressure balloon was specified to take place over 20 hours.

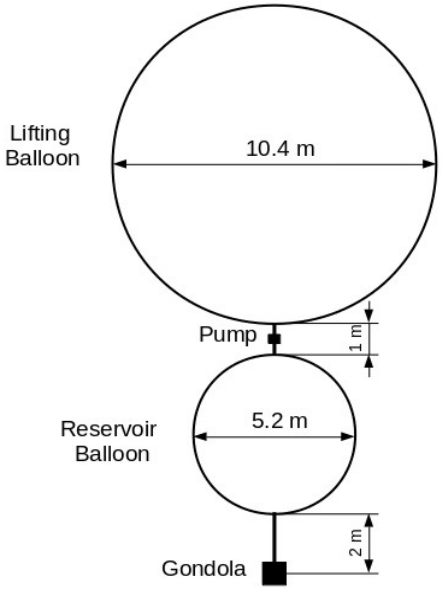

Figure 2: Schematic diagram of Pumped Helium tandem balloon model investigated in DSENDS simulation.

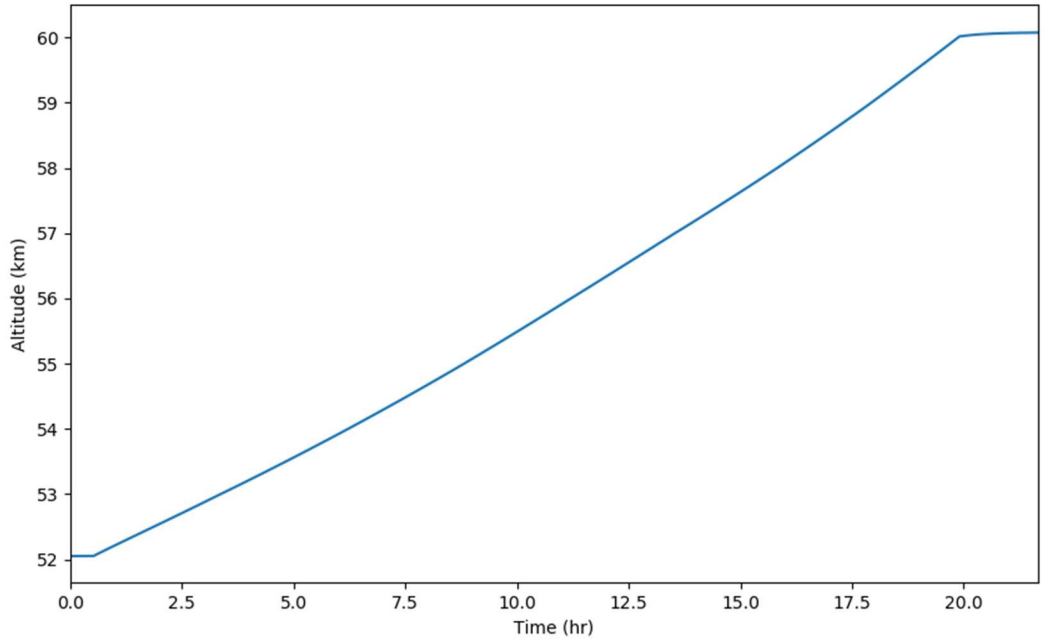

Figure 3: Ascent from 52 km up to 60 km over 20 hours

Note that the starting and ending altitudes are slightly off from 52 and 60 km due to the small effect of infrared fluxes and resulting thermal behavior of the balloons, something not accounted for in the earlier simplified neutral buoyancy calculations.

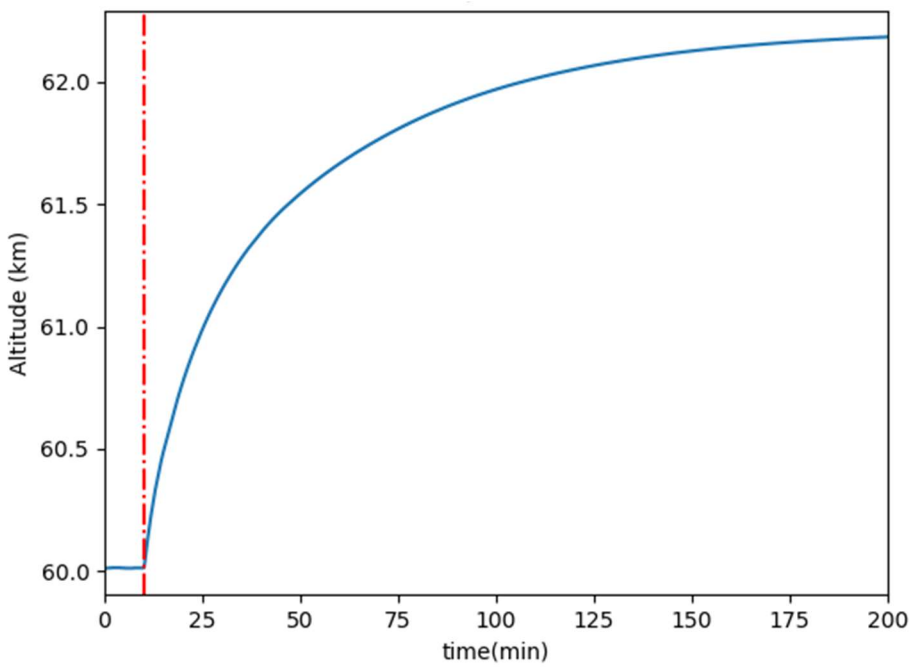

Figure 4: Vertical motion of tandem PH balloon with vertical updraft of 3 m/s starting at 10 minutes (denoted with the vertical red line)

In the second simulation, the tandem balloon system is at equilibrium and then encounters an updraft of 3 m/s starting at 10 minutes. See Figure 4 for the resulting behavior. The aerobot shows a rapid initial ascent that tapers off as the superpressure balloon generates less and less buoyancy in the lower density higher altitudes until an equilibrium is reached at 62.2 km. This displacement to 62.2 km is almost the same as the 62.1 km value estimated with the neutral buoyancy calculation as listed in Table 2. The time constant for this displacement to the new equilibrium is approximately 24 minutes if modeled as a first order system.

Conclusions

This paper analyzes variable altitude helium aerobots for the robotic exploration of Venus and Titan. Such balloon-based vehicles can provide a rich science return in future missions by providing atmospheric data across a wide altitude range and, in the case of Titan, conducting aerial reconnaissance of the surface and potentially acquiring and analyzing surface material. Altitude control also allows for the possibility of providing some amount of trajectory control on the principle that there can be different wind directions at different altitudes, a feature exploited with comparable terrestrial balloon vehicles such as the Google Loon and WorldView Stratolite.

Theoretical derivations for the limiting case of equal helium and atmospheric gas temperatures show two linear scaling relationships depending on the type of balloon. The superpressure linearly scales with atmospheric absolute temperature for the pumped helium and pumped air options, but scales linearly with atmospheric pressure for the mechanical compression option. Superpressure is therefore not a free design variable; if the superpressure is specified at one equilibrium altitude, it is determined for all altitudes.

Approximate point designs for specified Venus and Titan mission scenarios enable first order comparisons between the different aerobot concepts. The pumped helium aerobot option shows the lowest vehicle mass and lowest energy consumption for changing altitude in the selected Venus mission scenario, but with a high superpressure due to solar heating. The air ballast options are the heaviest and most energy intensive, with the mechanical compression balloon between these two extremes. The differences are significant, almost a factor of two in mass and a factor of five in energy between best and worst, and therefore serve as a clear discriminator. Future work is required to determine if these results can be generalized across the entire parameter space of design options for candidate Venus missions.

Titan balloons are roughly an order of magnitude less massive than Venus balloons due to the higher atmospheric density at the chosen flight altitudes and much lower superpressure levels. The low superpressure requirements for Titan also result in an order of magnitude smaller energy consumption compared to the Venus mission scenario. The Titan point design results show little difference between the different aerobot concepts on mass or energy consumption.

The DSENDS-based numerical simulation model presented in this paper provides the foundation to investigate other balloon topologies and more complex models. Preliminary calculations of a pumped helium balloon design show good agreement with the simplified neutral buoyancy calculations. In the future, as balloon designs evolve and mature, the DSENDS framework can be used to assess their performance in more complex time-varying simulations. Additionally, the DSENDS interface to sophisticated aerodynamic drag models enables investigating the effects of planetary wind currents and variable balloon morphologies.

Acknowledgements

The authors would like to acknowledge the editorial inputs and general encouragement of James Cutts of the Solar System Exploration Directorate Program Office at JPL. The research described in this paper was funded by the Jet Propulsion Laboratory, California Institute of Technology, under a contract with the National Aeronautics and Space Administration.

References

[1] Venus Aerial Platforms Study Team, "Aerial Platforms for the Scientific Exploration of Venus", JPL D-102569, October, 2018.
[2] https://loon.co/
[3] https://worldview.space/
[4] Voss, P. B., Riddle, E. E., and Smith, M. S. "Altitude control of long-duration balloons", *AIAA Journal of Aircraft*, Vol. 42, No. 2, pp 478-482, 2005.
[5] L. Blackmore, Y. Kuwata, M. Wolf, C. Assad, N. Farthpour, C. Newman, and A. Elfes, "Global Reachability and Path Planning for Planetary Exploration with Montgolfiere balloons," in IEEE Intl. Conf. on Robotics and Automation (ICRA), 2010.
[6] Jones, Jack A. and Heun, Matthew K. "Montgolfiere Balloon Aerobots For Planetary Atmospheres", AIAA Paper 97-1445.
[7] De Jong, Maxim, "Systems and Methods Including Elevation Control", United States Patent Application US 2017/0129579 A1, Assignee: Thin Red Line Aerospace Ltd., May 11, 2017.
[8] Sagdeev, R. Z., et al. "Overview of VEGA Balloon in Situ Meteorological Measurements", *Science*, **231**, p. 1411-1414, 1986.

[9] J. L. Hall, D. Fairbrother, T. Frederickson, V. V. Kerzhanovich, M. Said, C. Sandy, C. Willey and A. H. Yavrouian, "Prototype design and testing of a Venus long duration, high altitude balloon", Advances in Space Research, Vol. 42, pp 1648-1655, 2008.
[10] J. L. Hall, V. V. Kerzhanovich, A. H. Yavrouian, G. A. Plett, M. Said, D. Fairbrother, C. Sandy, T. Frederickson, G. Sharpe, and S. Day, "Second generation prototype design and testing for a high altitude Venus balloon", Advances in Space Research, Vol. 44, pp. 93-105, 2008.
[11] H. B. Niemann, S. K. Atreya, J. E. Demick, D. Gautier, J. A. Haberman, D. N. Harpold, W. T. Kasprzak, J. I. Lunine, T. C. Owen, and F. Raulin, "Composition of Titan's lower atmosphere and simple surface volatiles as measured by the Cassini-Huygens probe gas chromatograph mass spectrometer experiment", Journal of Geophysical Research, Vol. 115, E12006, 2010.
[12] J. L. Hall, V. V. Kerzhanovich, A. H. Yavrouian, J. A. Jones, C.V. White, B. A. Dudik, G. A. Plett, J. Mennella and A. Elfes. "An Aerobot For Global *In Situ* Exploration of Titan", *Advances in Space Research*, Vol. 37, pp 2108-2119, 2006.
[13] J. L. Hall, J. A. Jones, V. V. Kerzhanovich, T. Lachenmeier, P. Mahr, J. M. Mennella, M. Pauken, G. A. Plett, L. Smith, M. L. Van Luvender, A. H. Yavrouian. "Experimental results for Titan aerobot thermo-mechanical subsystem development", Advances in Space Research, Vol. 42, pp. 1641-1647, 2008.
[14] Cameron, J.M., Jain, A., Burkhart, P.D., Bailey, E.S., Balaram, B., Bonfiglio, E., Ivanov, M., Benito, J., Sklyanskiy, E. and Strauss, W., 2016. "DSENDS: Multi-mission Flight Dynamics Simulator for NASA Missions", p. 5421. In *AIAA SPACE 2016*.
[15] Cameron, J., Cutts, J., Jones, J., Wu, J., Raque, S. and Smith, I., "Versatile Modeling and Simulation Techniques for Earth and Planetary Balloon Systems", In AIAA Lighter-Than-Air Systems Technology Conference. 1999.
[16] Carlson, L.A. and Horn, W.J. "New Thermal and Trajectory Model for High-Altitude Balloons", J. Aircraft, Vol. 20, No. 6, June 1983.
[17] Serban, R. and Hindmarsh, A.C., "CVODES: the sensitivity-enabled ODE solver in SUNDIALS", In ASME 2005 international design engineering technical conferences and computers and information in engineering conference. pp. 257-269. American Society of Mechanical Engineers. January 2005.